Fermentative *Escherichia coli* makes a substantial contribution to H_2 production in coculture with phototrophic *Rhodopseudomonas palustris*

Amee A. Sangani[1,2†], Alexandra L. McCully[1,3†], Breah LaSarre[1], and James B. McKinlay[1]

[1]Department of Biology, Indiana University, Bloomington, IN

[2]Biology Undergraduate Program, Indiana University, Bloomington, IN

[3] Current address: Department of Civil and Environmental Engineering, Stanford University, CA

[†]Equal contributions.

*Corresponding author: James B. McKinlay, 1001 E 3rd St. Bloomington, IN 47405, Ph: 812-855-0359, Fax: 812-855-6705, Email: jmckinla@indiana.edu

Keywords: Coculture, Hydrogen, Biofuel, Cross-feeding, Syntrophy, Rhodopseudomonas palustris, Formate hydrogenlyase

Abstract

Individual species within microbial communities can combine their attributes to produce services that benefit society, such as the transformation of renewable resources into valuable chemicals. Under defined genetic and environmental conditions, fermentative *Escherichia coli* and phototrophic *Rhodopseudomonas palustris* exchange essential carbon and nitrogen, respectively, to establish a mutualistic relationship. In this relationship, each species produces H_2 biofuel as a byproduct of their metabolism. However, the extent to which each species contributes to H_2 production and the factors that influence their relative contributions were previously unknown. By comparing H_2 yields in cocultures pairing *R. palustris* with either wild-type *E. coli* or a formate hydrogenlyase mutant that is incapable of H_2 production, we determined the relative contribution of each species to total H_2 production. Our results indicate that *E. coli* contributes between 32% and 86% of the H_2 produced in coculture depending on the level of ammonium excreted by the *R. palustris* partner. An *R. palustris* strain that stimulated rapid *E. coli* growth through a high level of ammonium excretion resulted in earlier accumulation of formate and acidic conditions that allowed *E. coli* to be the major contributor to H_2 production.

Introduction

The collective activities of microbial communities can be harnessed to benefit society in ways ranging from the degradation of pollutants to the production of valuable chemicals and fuels (Zuroff & Curtis, 2012, Johns *et al.*, 2016, Cavaliere *et al.*, 2017). Synthetic communities (i.e., cocultures) pairing fermentative and phototrophic purple nonsulfur bacteria have long been viewed as an attractive means by which to convert carbohydrates to hydrogen gas (H_2) biofuel (Odom & Wall, 1983). In such communities, fermentative bacteria often dedicate some electrons extracted from carbohydrates to H_2 production, but most of the electrons end up in excreted

organic acids and alcohols. Purple nonsulfur bacteria can use energy from light to access electrons in fermentation products and use these electrons for both biosynthesis and H_2 production, thereby increasing the total H_2 yield. While the advantages of such communities for achieving a higher H_2 yield in a consolidated process have long been known (Odom & Wall, 1983), the contributions of each species to H_2 production and the underlying microbial interactions have been difficult to characterize due to a lack of reproducibility and tractability in these communities.

We previously developed a highly reproducible and tractable coculture between fermentative *Escherichia coli* and the purple nonsulfur bacterium, *Rhodopseudomonas palustris* (LaSarre *et al.*, 2017). As in previous cocultures of this kind, *E. coli* ferments glucose into excreted organic acids and ethanol. One organic acid, formate, can be further converted by *E. coli* into H_2 and CO_2 via formate hydrogenlyase (FHL) (Pinske & Sawers, 2016). Formate cannot be metabolized by *R. palustris*, but *R. palustris* readily consumes the other organic acids, namely acetate, lactate, and succinate. *R. palustris* does not metabolize sugars and is thus reliant on *E. coli* for the carbon and electrons in these organic acids (LaSarre *et al.*, 2017). Stable coexistence of the species in coculture is assured by requiring that *E. coli* rely on *R. palustris* for essential nitrogen. This dependency is achieved by (i) providing N_2 gas as the sole nitrogen source, as only *R. palustris* can convert N_2 into NH_4^+ via nitrogenase, and (ii) by using *R. palustris* mutants that excrete NH_4^+ as a nitrogen source for *E. coli* (LaSarre *et al.*, 2017). These conditions also drive H_2 production by *R. palustris*, as H_2 an obligate byproduct of the nitrogenase reaction.

Here we use an *E. coli* mutant lacking FHL activity to assess the contribution of each species to H_2 production in coculture. We find that either species can make the majority contribution to H_2 production depending on the level of NH_4^+ excreted by the *R. palustris* partner. A highly cooperative *R. palustris* partner, exhibiting a high level of NH_4^+ excretion, leads to conditions that result in *E. coli* being the major contributor to H_2 production.

Materials and Methods

Strains and growth conditions. All *R. palustris* strains were derived from the type strain CGA009 (Larimer *et al.*, 2004). *R. palustris* Nx (CGA4005) has a *nifA* mutation that results in NH_4^+ excretion during N_2 fixation, a *hupS* deletion to prevent H_2 oxidation, and a *uppE* deletion that prevents biofilm formation (Fritts *et al.*, 2017, LaSarre *et al.*, 2017). *R. palustris* NxΔAmtB (CGA4021) has the same mutations as the Nx strain and additional *amtB1* and *amtB2* deletions that result in 3-fold more NH_4^+ excretion than the Nx strain (LaSarre *et al.*, 2017). *E. coli* MG1655 was the wild-type (WT) strain (Blattner *et al.*, 1997). The ΔFdhF strain was created by transferring the *ΔfdhF*::Km^R mutation from *E. coli* JW4040 (Baba *et al.*, 2006) into *E. coli* MG1655 using P1 phage transduction (Thomason *et al.*, 2007). Mutants were selected on LB agar with 30 µg/mL kanamycin and were verified by PCR. Empty vector (pCA24N) and the complementation vector (pCA24N_fdhF) (Kitagawa *et al.*, 2005) were electroporated into *E. coli* ΔFdhF and transformants were selected on LB agar with 25 µg/mL chloramphenicol. Monocultures and cocultures were grown in 10 mL of M9-derived coculture (MDC) medium (LaSarre *et al.*, 2017) in 27-mL anaerobic test tubes. Where appropriate, MOPS was added during the preparation of MDC medium using a 1M stock at pH 7 for a final concentration of 100 mM. Tubes were made anaerobic by bubbling with N_2 and were then sealed with rubber stoppers and aluminum crimps, creating a headspace of 100% N_2. MDC medium was

supplemented with 1% v/v cation solution (100 mM $MgSO_4$, 10 mM $CaCl_2$) and 25 mM glucose. For *E. coli* monocultures, 15 mM NH_4Cl was added. All anaerobic cultures were grown at 30°C, lying flat with shaking at 150 rpm beneath a 60 W incandescent bulb. Starter monocultures and cocultures were inoculated from single colonies suspended in 0.2 ml of MDC. Once fully grown, 0.1 mL of starter culture was inoculated into test conditions.

Analytical Procedures. Cell densities were quantified by optical density at 660nm (OD_{660}) using a Genesys 20 spectrophotometer (Thermo-Fisher). Growth curves used cell densities measured in the culture tubes. Growth rates were determined using values between 0.1 and 1.0 OD_{660} where there is linear correlation between OD_{660} and cell density. Growth yields were determined using OD_{660} values from initial and final time points measured in cuvettes, with samples diluted into the linear range as necessary. Glucose and soluble fermentation products were quantified using a Shimadzu high-performance liquid chromatograph as described (McKinlay *et al.*, 2005). H_2 was quantified using a Shimadzu gas chromatograph as described (Huang *et al.*, 2010). To determine final pH values, whole cultures were centrifuged, the supernatants passed through 0.2 µm syringe filters, and the pH of the filtrate measured using a pH meter.

Results

Formate dehydrogenase-H is required for H_2 production by *E. coli*. In cocultures pairing WT *E. coli* with *R. palustris* Nx, a mutant that excretes NH_4^+ during N_2 fixation, both species are presumed to produce H_2 (Fig 1). However, the contribution of each species to H_2 production was unknown. To determine the contribution of each species to H_2 production, we genetically disrupted H_2 production in *E. coli*. We did not attempt to disrupt H_2 production in *R. palustris* because H_2 is an obligate byproduct of nitrogenase during the conversion of N_2 to NH_4^+; consequently, *R. palustris* H_2 production cannot be eliminated without simultaneously disrupting the NH_4^+ cross-feeding that underpins the mutualism. In *E. coli*, H_2 is produced by the FHL complex, composed of formate dehydrogenase-H and hydrogenase-3, which converts formate to H_2 and CO_2 (Pinske & Sawers, 2016). Unlike other *E. coli* fermentation products, formate is not consumed by *R. palustris* (Fig. 1).

It is well-known that *fdhF*, encoding formate dehydrogenase-H, is required for H_2 production by *E. coli* (Pinske & Sawers, 2016). We therefore deleted *fdhF*, resulting in strain ΔFdhF, and examined the effects of the *fdhF* deletion on fermentative growth and metabolic trends in monoculture. The growth curves of WT and ΔFdhF *E. coli* monocultures were comparable (Fig. 2A), as were the growth yields (Fig. 2B) and growth rates (Fig. 2C). As expected, the ΔFdhF mutant did not produce any detectable H_2 and had a higher formate yield than did the WT strain (Fig. 2D). Other fermentation product yields were comparable in the WT and ΔFdhF cultures (Fig. 2D). We verified that the loss of H_2 production and higher formate yield in the ΔFdhF cultures were due to the lack of the *fdhF* gene and not due to polar effects of the deletion by complementing the ΔFdhF mutant with a plasmid bearing *fdhF* under an IPTG-inducible promoter (pCA24N_fdhF). Whereas the empty vector had no effect on product yields, complementation with pCA24N_fdhF restored H_2 production and resulted in formate yields similar to WT levels (Fig. 2D). Complementation with pCA24N_fdhF also resulted in a higher lactate yield than the WT strain (Fig. 2D), though the reasons for this trend are not obvious. Because formate accumulation can acidify the culture medium we also measured the culture pH once growth had ceased. Despite the higher formate level in ΔFdhF cultures, there was no

significant difference in final culture pH compared to WT cultures (Fig. 2E). Overall, all results verified that deletion of *fdhF* abolishes H_2 production with a concomitant increase in formate yield but without affecting other growth and metabolic trends.

***E. coli* contributes to H_2 production in coculture with *R. palustris*.** As deletion of *fdhF* abolished the conversion of formate to H_2 by *E. coli* without altering other growth or metabolic trends, we deemed the ΔFdhF mutant suitable for assessing the contribution of *E. coli* to H_2 production in coculture. We grew the ΔFdhF mutant with *R. palustris* Nx (i.e., Nx+ΔFdhF coculture) and compared growth and metabolic trends to cocultures pairing *R. palustris* Nx with WT *E. coli* (i.e., Nx+WT coculture). We observed no significant differences in the growth trends between the Nx+WT and Nx+ΔFdhF cocultures (Fig. 3A-C). The H_2 yield in Nx+ΔFdhF cocultures was significantly lower than that of Nx+WT cocultures, whereas the formate yield was significantly higher (Fig. 3D). Despite that formate yields were significantly higher in Nx+ΔFdhF cocultures, the final pH was still similar to that of Nx+WT cocultures (Fig. 3E). Since all growth and metabolic trends we assayed were statistically similar between the Nx+WT and Nx+ΔFdhF cocultures, except for formate and H_2 yields, we reasoned that the formate and H_2 yields were unlikely to be influenced in any major way by factors other than the absence of *fdhF*. Thus, we estimated the contribution of *E. coli* to H_2 production in coculture to be the difference in the H_2 yield between the Nx+WT and Nx+ΔFdhF cocultures. From this difference, we estimated that *E. coli* produces 32±5% (SD) of the H_2 in an Nx+WT coculture.

Higher NH_4^+ excretion by *R. palustris* results in a larger *E. coli* contribution to H_2 production. In the above cocultures with *R. palustris* Nx, the growth rates of the two species are coupled (LaSarre *et al.*, 2017). Consequently, *E. coli* grows at ~20% of the growth rate that would be possible if NH_4^+ were saturating, decreasing the rate of formate accumulation and acidification of the culture medium (LaSarre *et al.*, 2017). However, it is possible to uncouple the growth rates and allow *E. coli* to grow faster by growing *E. coli* with the hyper-cooperative *R. palustris* NxΔAmtB strain (LaSarre *et al.*, 2017). *R. palustris* NxΔAmtB lacks high-affinity AmtB transporters responsible for NH_4^+ import and thus excretes 3-times more NH_4^+ than does *R. palustris* Nx (LaSarre *et al.*, 2017). The higher level of NH_4^+ cross-feeding increases the *E. coli* growth rate in coculture and causes the rate of organic acid production by *E. coli* to exceed the rate of organic acid consumption by *R. palustris*. As a result, consumable organic acids accumulate along with formate and prematurely acidify the coculture and inhibit *R. palustris* growth unless the buffering capacity of the medium is raised. However, even without additional buffer, the coculture maintains reproducible trends through serial transfers (LaSarre *et al.*, 2017). The conversion of formate to H_2 and CO_2 by *E. coli* FHL requires anaerobic conditions and a pH below 7 and is influenced by the formate concentration (Rossmann *et al.*, 1991, Pinske & Sawers, 2016). Thus, we hypothesized that the faster growth of *E. coli* in coculture with *R. palustris* NxΔAmtB, and the associated acceleration of culture acidification and formate accumulation, might trigger earlier FHL activity and thereby increase *E. coli's* contribution to H_2 production.

We compared growth and metabolic trends in cocultures pairing *R. palustris* NxΔAmtB with either WT *E. coli* (NxΔAmtB+WT) or the ΔFdhF mutant (NxΔAmtB+ΔFdhF). Again, growth trends in cocultures with *R. palustris* NxΔAmtB were not significantly affected by the absence of *E. coli fdhF* (Fig. 4A-C). As expected, compared to cocultures with *R. palustris* Nx, cocultures

with *R. palustris* NxΔAmtB reached stationary phase more quickly (Fig. 3A vs. Fig 4A) due to the increased growth rate of *E. coli* (LaSarre *et al.*, 2017). To take into account the shortened growth period of *R. palustris* NxΔAmtB-containing cocultures in our comparisons with *R. palustris* Nx-containing cocultures, we sampled *R. palustris* NxΔAmtB-containing cocultures at two time points: (i) 96 h, which roughly matches the time that *R. palustris* Nx-containing cocultures spent in stationary phase; and (ii) 167 h, which corresponds to the total time for coculture experiments with *R. palustris* Nx.

As observed previously (LaSarre *et al.*, 2017), consumable organic acids accumulated in cocultures with *R. palustris* NxΔAmtB (Fig. 4D). The average H_2 yield of the NxΔAmtB+ΔFdhF cocultures across both time points was 0.10±0.01 mol/mole glucose (Fig. 4D), which is approximately one-third of that of the Nx+ΔFdhF cocultures (Fig. 3D). This H_2 yield, which reflects the contribution by *R. palustris* NxΔAmtB, is likely low due to the inhibition of *R. palustris* growth and metabolism by acidification of the coculture before all consumable organic acids could be consumed (Fig. 4D and E), as observed previously (LaSarre *et al.*, 2017). In contrast, the NxΔAmtB+WT cocultures showed an increasing H_2 yield between the two time points, eventually reaching levels comparable to those observed in Nx+WT cocultures (Fig. 4D). Taking the difference between the H_2 yields of the NxΔAmtB+ΔFdhF and the NxΔAmtB+WT cocultures, we estimated that *E. coli* contributed 70±20 % and 86±26 % of the total H_2 observed at 96 and 167 hours, respectively. Thus, unlike in Nx+WT cocultures, *E. coli* generated the majority of the H_2 in NxΔAmtB+WT cocultures. This higher percent contribution by *E. coli* to H_2 production was due in part to inhibition of *R. palustris*, but it was also due to *E. coli* having produced 2.4-times as much H_2 per glucose in cocultures with *R. palustris* NxΔAmtB than in cocultures with *R. palustris* Nx (Fig. 5).

The increase in H_2 yield between time points in NxΔAmtB+WT cocultures corresponded with a decrease in the formate yield (Fig. 4D), indicating conversion of formate into H_2 by WT *E. coli*. This formate removal also explains why the pH was higher in NxΔAmtB+WT cocultures compared to NxΔAmtB+ΔFdhF cocultures (Fig. 4E). The final pH of the NxΔAmtB+WT cocultures was also higher than that observed in a previous study on NxΔAmtB+WT cocultures (LaSarre *et al.*, 2017). Again, this difference is likely due to the removal of additional formate during the prolonged incubation; in the current study we sacrificed cultures to measure pH at 167 h (Fig. 4E), whereas previously we sacrificed cultures to measure pH at 96 h (LaSarre *et al.*, 2017). The extended incubation time and difference in the final pH between the two cocultures might also explain why the lactate yield was higher in the NxΔAmtB+ΔFdhF cocultures, because a low pH and fermentative conditions are known to stimulate lactate dehydrogenase activity in *E. coli* (Mat-Jan *et al.*, 1989, Jiang *et al.*, 2001).

The acidification of the medium in cocultures with *R. palustris* NxΔAmtB leaves some electron-containing organic acids unconsumed that *R. palustris* could otherwise convert to H_2 via nitrogenase. To determine how much additional H_2 could be made if *R. palustris* NxΔAmtB was not inhibited by the low pH, we repeated the experiments in medium supplemented with 100 mM MOPS, pH 7. This additional MOPS was not expected to inhibit *E. coli* FHL activity given that the pH of the medium without MOPS also has at a pH of 7, and both media acidify as *E. coli* grows fermentatively. Growth trends were similar between NxΔAmtB+WT and NxΔAmtB+ΔFdhF cocultures supplemented with MOPS (Fig. 6A-C). The presence of

consumable organic acids at 94 h indicated that *E. coli* again grew rapidly and produced organic acids faster than *R. palustris* could consume them (Fig. 6D). However, the mildly acidic pH, only reaching 6.5 at 164 h (Fig. 6E), allowed *R. palustris* to eventually metabolize nearly all consumable organic acids (Fig. 6D). From the difference in H_2 yields between MOPS-supplemented NxΔAmtB+WT and NxΔAmtB+ΔFdhF cocultures, we estimated that *E. coli* generated 63±10% of the H_2 in cocultures at 94 h, similar to the *E. coli* contribution at 96 hours in Nx+WT cocultures (Fig. 4D). Thus, the additional MOPS buffer did not have a major inhibitory effect on FHL activity. By 164 h, the *E. coli* H_2 contribution increased to 69±6% of the H_2 produced, even though both species generated H_2 during this time; for comparison, the H_2 yield increased 1.4-fold between 94 and 164 h due to *R. palustris* nitrogenase activity alone in NxΔAmtB+ΔFdhF cocultures (Fig. 4D). The lower percentage of H_2 contributed by *E. coli* in MOPS-supplemented NxΔAmtB+ΔFdhF cocultures compared to cocultures without MOPS was a result of increased H_2 production by *R. palustris* NxΔAmtB, as the *E. coli* H_2 yield was estimated to be similar in NxΔAmtB+ΔFdhF cocultures with and without MOPS (Fig. 5). As *R. palustris* NxΔAmtB was not the major H_2 contributor even when allowed to fully consume the consumable organic acids, we conclude that the early exposure of *E. coli* to formate under FHL-activating conditions allows *E. coli* to make a greater contribution to H_2 production than *R. palustris* in NxΔAmtB+WT cocultures. However, one reason that *R. palustris* NxΔAmtB did not make as much H_2 in MOPS-supplemented cocultures compared to *R. palustris* Nx in coculture is because *R. palustris* NxΔAmtB shifted the *E. coli* fermentation balance towards ethanol, increasing the ethanol yield more than 2-fold above that observed in Nx+WT cocultures (Fig. 3D vs Fig. 4D and 6D). Because *R. palustris* does not consume ethanol in coculture, the high ethanol yield detracted from the electrons that *R. palustris* could otherwise have devoted to H_2 production.

Discussion

Our results indicate that *E. coli* can make a substantial contribution to H_2 production in cocultures with *R. palustris,* with the contribution ranging from 32-86% depending on the level of NH_4^+ excretion by the *R. palustris* partner and the length of time that *E. coli* is exposed to formate. Even in Nx+WT cocultures, wherein *E. coli* contributed the least (~32%) to H_2 production (Fig. 3D), the contribution was still considerable in view of the fact that *E. coli* makes up only ~10% of the total population (LaSarre *et al.*, 2017, McCully *et al.*, 2017). This large contribution of *E. coli* to H_2 on a 'per cell' basis reflects the difference in how electrons are managed in fermentation versus in photoheterotrophic growth. During fermentation, most of the electrons are disposed of in fermentation products, including H_2, to satisfy electron balance. During photoheterotrophic growth by *R. palustris*, H_2 production also contributes to electron balance, but most of the electrons are incorporated into new cell material (McKinlay & Harwood, 2010, McKinlay & Harwood, 2011). Thus, the relative biosynthetic efficiency of each species' lifestyle plays a large role in determining its respective contributions to H_2 production.

The H_2 contribution by *E. coli* was greater in cocultures with *R. palustris* NxΔAmtB, in which the conditions required for *E. coli* FHL activity were established relatively early, thereby prolonging the period over which *E. coli* could convert formate to H_2 (Fig. 4D and 6D). The greater *E. coli* contribution to H_2 yields in NxΔAmtB+WT cocultures compared to that in Nx+WT cocultures could also be due in part to a larger *E. coli* population; *E. coli* makes up 30-50% of the total population in NxΔAmtB+WT cocultures, with absolute *E. coli* populations

being ~2-fold larger in NxΔAmtB+WT cocultures compared to Nx+WT cocultures (LaSarre *et al.*, 2017, McCully *et al.*, 2017).

The results herein could contribute to the rational design of H_2-producing communities. Much research has focused on the potential use of purple nonsulfur bacteria to convert fermented agricultural or municipal waste into H_2. Coculture systems like ours can be viewed as a precursor for a consolidated process in which purple nonsulfur bacteria, like *R. palustris*, would be integrated with a fermentative community in situ. In our coculture, *E. coli* serves as a proxy for a fermentative community. While not all fermentative microbes generate H_2 (Odom & Wall, 1983), our results show that fermentative bacteria could be major contributors to H_2 production in communities with purple nonsulfur bacteria. Although the highest H_2 yield observed in our study was 0.6 mol H_2/mol glucose, or 5% of the theoretical maximum yield, it is possible that the yield would be higher if more time were allowed for *E. coli* to convert remaining formate into H_2. Continuous removal of H_2 from the headspace could also improve H_2 production by relieving thermodynamic feedback on hydrogenase activity (Mandal *et al.*, 2006). It is also possible that the *R. palustris* contribution to H_2 production could be increased by integrating *R. palustris* into a fermentative community in a manner where its access to nitrogen could be controlled, for example, using a latex biofilm (Gosse *et al.*, 2007, Gosse *et al.*, 2010, McKinlay & Harwood, 2010). We previously observed that nitrogen-starved *R. palustris* suspensions produced H_2 at yields as high 66% of the theoretical maximum (McKinlay *et al.*, 2014). Similarly, in nitrogen-limited cocultures we observed an H_2 yield of >4 mol H_2/mol glucose, or 33% of the theoretical maximum yield (McCully *et al.*, 2017). Overall, our results illustrate how synthetic tractable communities can be used to inform on the design and application of microbial communities to benefit society.

Funding. This work was supported by the U.S. Army Research Office, grant W911NF-14-1-04. AAS was supported by Indiana University's Cox Research Scholars Program and the Hutton Honors College.

References.

Baba T, Ara T, Hasegawa M, Takai Y, Okumura Y, Baba M, Datsenko KA, Tomita M, Wanner BL & Mori H (2006) Construction of *Escherichia coli* K-12 in-frame, single-gene knockout mutants: the Keio collection. Mol Syst Biol 2: 2006 0008.

Blattner FR, Plunkett G, 3rd, Bloch CA, et al. (1997) The complete genome sequence of *Escherichia coli* K-12. Science 277: 1453-1462.

Cavaliere M, Feng S, Soyer OS & Jimenez JI (2017) Cooperation in microbial communities and their biotechnological applications. Environ Microbiol 19: 2949-2963.

Fritts RK, LaSarre B, Stoner AM, Posto AL & McKinlay JB (2017) A *Rhizobiales*-specific unipolar polysaccharide adhesin contributes to *Rhodopseudomonas palustris* biofilm formation across diverse photoheterotrophic conditions. Appl Environ Microbiol 83: e03035-16.

Gosse JL, Engel BJ, Hui JC, Harwood CS & Flickinger MC (2010) Progress toward a biomimetic leaf: 4,000 h of hydrogen production by coating-stabilized nongrowing photosynthetic *Rhodopseudomonas palustris*. Biotechnol Prog 26: 907-918.

Gosse JL, Engel BJ, Rey FE, Harwood CS, Scriven LE & Flickinger MC (2007) Hydrogen production by photoreactive nanoporous latex coatings of nongrowing *Rhodopseudomonas palustris* CGA009. Biotechnol Prog 23: 124-130.

315 Huang JJ, Heiniger EK, McKinlay JB & Harwood CS (2010) Production of hydrogen gas from light
316 and the inorganic electron donor thiosulfate by *Rhodopseudomonas palustris*. Appl Environ
317 Microbiol 76: 7717-7722.
318 Jiang GR, Nikolova S & Clark DP (2001) Regulation of the ldhA gene, encoding the fermentative
319 lactate dehydrogenase of *Escherichia coli*. Microbiology 147: 2437-2446.
320 Johns NI, Blazejewski T, Gomes AL & Wang HH (2016) Principles for designing synthetic
321 microbial communities. Curr Opin Microbiol 31: 146-153.
322 Kitagawa M, Ara T, Arifuzzaman M, Ioka-Nakamichi T, Inamoto E, Toyonaga H & Mori H (2005)
323 Complete set of ORF clones of *Escherichia coli* ASKA library (a complete set of E. coli K-12 ORF
324 archive): unique resources for biological research. DNA Res 12: 291-299.
325 Larimer FW, Chain P, Hauser L, et al. (2004) Complete genome sequence of the metabolically
326 versatile photosynthetic bacterium *Rhodopseudomonas palustris*. Nat Biotechnol 22: 55-61.
327 LaSarre B, McCully AL, Lennon JT & McKinlay JB (2017) Microbial mutualism dynamics
328 governed by dose-dependent toxicity of cross-fed nutrients. ISME J 11: 337-348.
329 Mandal B, Nath K & Das D (2006) Improvement of biohydrogen production under decreased partial
330 pressure of H_2 by *Enterobacter cloacae*. Biotechnol Lett 28: 831-835.
331 Mat-Jan F, Alam KY & Clark DP (1989) Mutants of *Escherichia coli* deficient in the fermentative
332 lactate dehydrogenase. J Bacteriol 171: 342-348.
333 McCully AL, LaSarre B & McKinlay JB (2017) Growth-independent cross-feeding modifies
334 boundaries for coexistence in a bacterial mutualism. Environ Microbiol 19: 3538-3550.
335 McCully AL, LaSarre B & McKinlay JB (2017) Recipient-biased competition for a cross-fed nutrient
336 is required for coexistence of microbial mutualists. mBio 8: e01620-17
337 McKinlay JB & Harwood CS (2010) Photobiological production of hydrogen gas as a biofuel. Curr
338 Opin Biotechnol 21: 244-251.
339 McKinlay JB & Harwood CS (2010) Carbon dioxide fixation as a central redox cofactor recycling
340 mechanism in bacteria. Proc Natl Acad Sci U S A 107: 11669-11675.
341 McKinlay JB & Harwood CS (2011) Calvin cycle flux, pathway constraints, and substrate oxidation
342 state together determine the H_2 biofuel yield in photoheterotrophic bacteria. mBio 2:
343 e00323-10
344 McKinlay JB, Zeikus JG & Vieille C (2005) Insights into *Actinobacillus succinogenes* fermentative
345 metabolism in a chemically defined growth medium. Appl Environ Microbiol 71: 6651-6656.
346 McKinlay JB, Oda Y, Ruhl M, Posto AL, Sauer U & Harwood CS (2014) Non-growing
347 *Rhodopseudomonas palustris* increases the hydrogen gas yield from acetate by shifting from the
348 glyoxylate shunt to the tricarboxylic acid cycle. J Biol Chem 289: 1960-1970.
349 Odom JM & Wall JD (1983) Photoproduction of H_2 from cellulose by an anaerobic bacterial
350 coculture. Appl Environ Microbiol 45: 1300-1305.
351 Pinske C & Sawers RG (2016) Anaerobic formate and hydrogen metabolism. EcoSal Plus 7.
352 Rossmann R, Sawers G & Bock A (1991) Mechanism of regulation of the formate-hydrogenlyase
353 pathway by oxygen, nitrate, and pH: definition of the formate regulon. Mol Microbiol 5: 2807-2814.
354 Thomason LC, Costantino N & Court DL (2007) *E. coli* genome manipulation by P1 transduction.
355 Curr Protoc Mol Biol Chapter 1: Unit 1 17.
356 Zuroff TR & Curtis WR (2012) Developing symbiotic consortia for lignocellulosic biofuel
357 production. Appl Microbiol Biotechnol 93: 1423-1435.
358
359
360
361
362

Figures

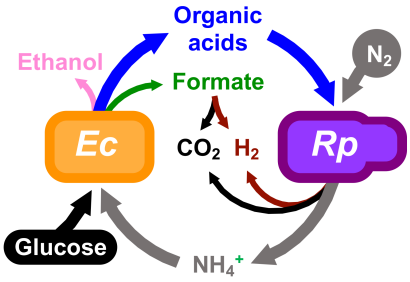

Fig. 1. A mutualistic H_2-producing coculture between WT *E. coli (Ec)* and *R. palustris (Rp)* Nx. *E. coli* ferments glucose into organic acids that serve as an essential carbon source for *R. palustris*. Ethanol and formate accumulate, but WT *E. coli* can convert formate into H_2 and CO_2 using FHL. *R. palustris* Nx converts N_2 gas into NH_4^+ via nitrogenase and excretes some NH_4^+ that serves as an essential nitrogen source for *E. coli*. *R. palustris* produces H_2 as a byproduct of the nitrogenase reaction.

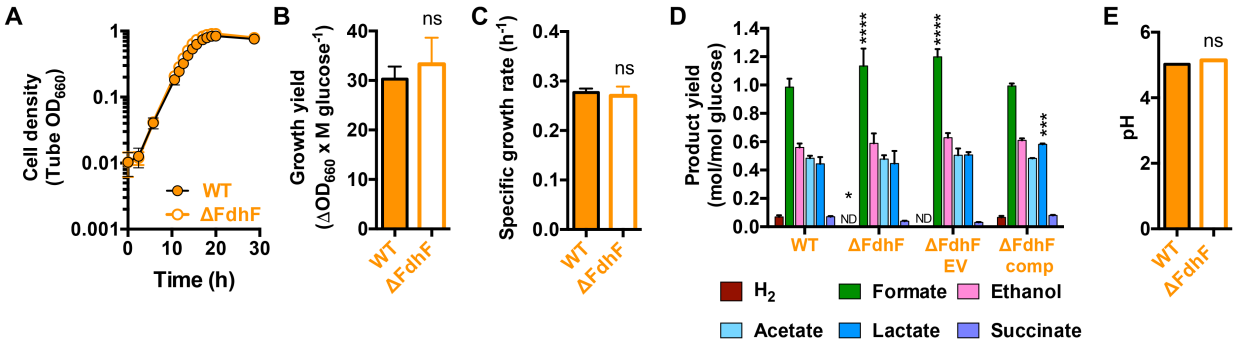

Fig. 2. Growth and metabolic trends of WT *E. coli* and ΔFdhF mutant monocultures. Growth curves (n=3) (A), growth yields (n=6) (B), and growth rates (n=3) (C) of WT and ΔFdhF *E. coli* strains. (D) Fermentation product yields(n=6). Asterisks indicate a statistical difference from corresponding WT value with P<0.05 (*), P<0.001 (***), P<0.0001 (****), determined by two-way ANOVA with Sidak posttest. EV, empty vector (pCA24N); comp, complementation vector (pCA24N_fdhF). (E) Final pH (n=3). (A-E) Error bars, SD. (B, C, E) Statistical differences from WT trends were determined using an unpaired, two-tailed t test; ns, non-significant.

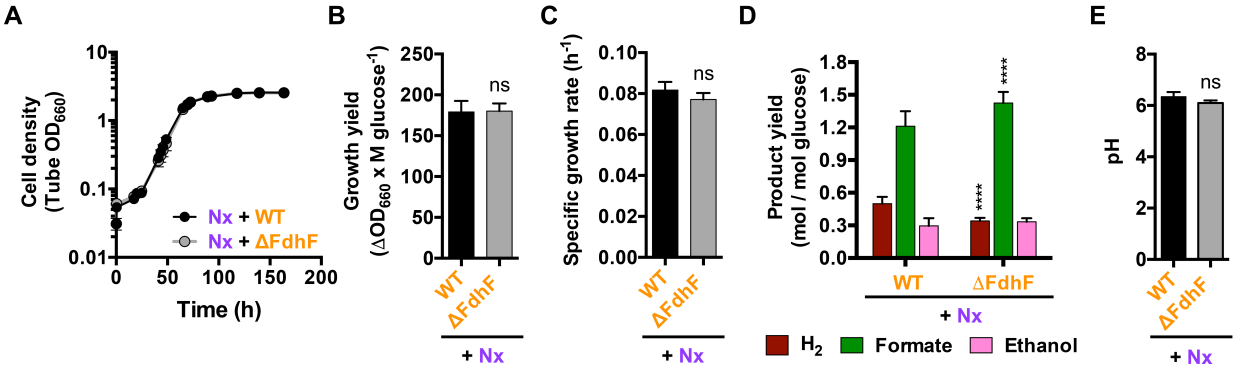

Fig. 3. Growth and metabolic trends of cocultures pairing *R. palustris* Nx with either WT *E. coli* or the ΔFdhF mutant. Coculture growth curves (A), growth yields (B), growth rates (C), product yields (D), and final pH (E) (n=3). (D) Acetate, lactate, and succinate were not detected, as these organic acids are consumed by *R. palustris* Nx (LaSarre *et al.*, 2017). ****, statistical difference from corresponding Nx+WT value (P<0.0001), determined by two-way ANOVA with Sidak posttest. (A-E) Error bars, SD. (B, C, E) Statistical differences were determined using an unpaired, two-tailed t test; ns, non-significant.

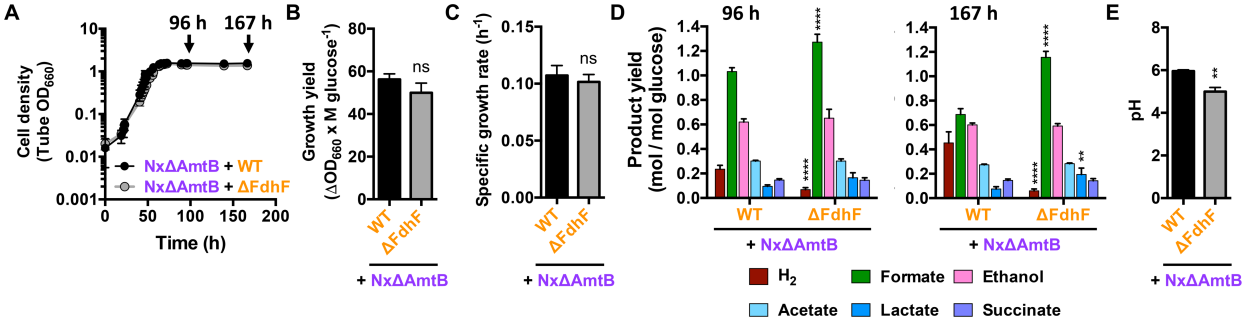

Fig. 4. Growth and metabolic trends of cocultures pairing *R. palustris* NxΔAmtB with either WT *E. coli* or the ΔFdhF mutant. Coculture growth curves (A), growth yields (B), growth rates (C), product yields (D), and final pH (E) (n=3). (D) Asterisks indicate a statistical difference from the corresponding NxΔAmtB+WT value, with P<0.0001 (****) or P<0.01 (**), determined by two-way ANOVA with Sidak posttest. (A-E) Error bars, SD. (B, C, E) Statistical differences were determined using an unpaired, two-tailed t test; ns, non-significant; P<0.01 (**).

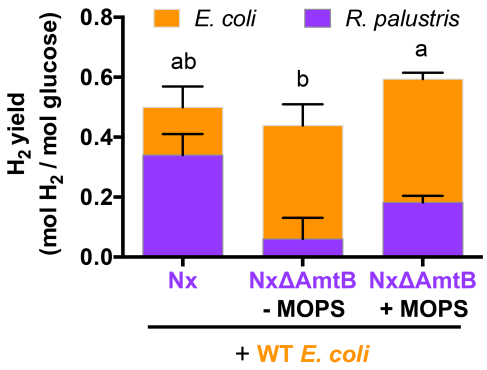

Fig. 5. Species-level comparison of H_2 yields in coculture. Yields were determined at the final time points shown in Figures 3, 4, and 6. The contribution of each species is estimated from the difference between cocultures with WT *E. coli,* which produces H_2, and those with *E. coli* ΔFdhF, which does not produce H_2. Different letters indicate a statistical difference between total H_2 yields ($P<0.05$), determined using one-way ANOVA with Tukey's multiple comparisons posttest.

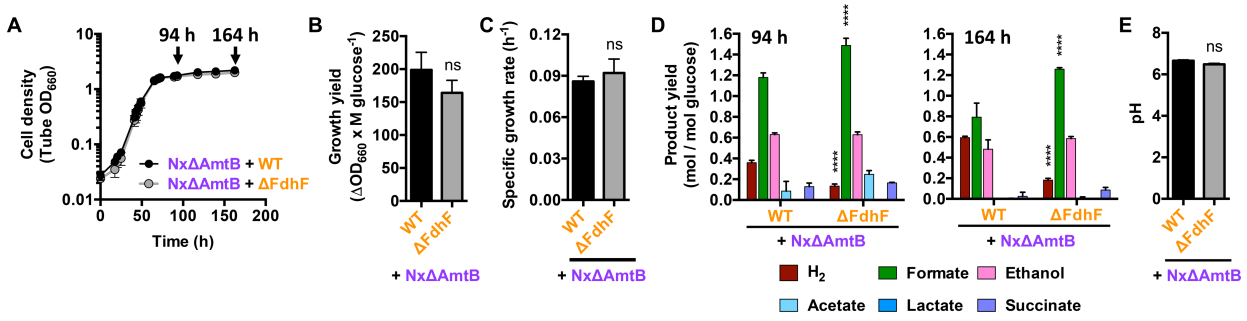

Fig. 6. Growth and metabolic trends of cocultures pairing *R. palustris* NxΔAmtB with either WT *E. coli* or the ΔFdhF mutant in medium supplemented with 100 mM MOPS, pH 7. Coculture growth curves (A), growth yields (B), growth rates (C), product yields (D), and final pH (E) (n=3). (D) Asterisks indicate a statistical difference from the corresponding NxΔAmtB+WT value, with $P<0.0001$ (****), determined by two-way ANOVA with Sidak posttest. (A-E) Error bars, SD. (B, C, E) Statistical differences were determined using an unpaired, two-tailed t test; ns, non-significant.